Suppression of the γ–α structural phase transition in $Ce_{0.8}La_{0.1}Th_{0.1}$ by large magnetic fields

2005 J. Phys.: Condens. Matter 17 L77

(http://iopscience.iop.org/0953-8984/17/7/L01)

INSTITUTE OF PHYSICS PUBLISHING JOURNAL OF PHYSICS: CONDENSED MATTER

J. Phys.: Condens. Matter **17** (2005) L77–L83 doi:10.1088/0953-8984/17/7/L01

LETTER TO THE EDITOR

Suppression of the γ–α structural phase transition in $Ce_{0.8}La_{0.1}Th_{0.1}$ by large magnetic fields

F Drymiotis[1], J Singleton[1], N Harrison[1], J C Lashley[1], A Bangura[2], C H Mielke[1], L Balicas[3], Z Fisk[4], A Migliori[1] and J L Smith[1]

[1] Los Alamos National Laboratory, Los Alamos, NM87545, USA
[2] Condensed Matter Physics, Department of Physics, University of Oxford, The Clarendon Laboratory, Parks Road, Oxford OX1 3PU, UK
[3] National High Magnetic Field Laboratory, 1800 E Paul Dirac Drive, Tallahassee, FL32310, USA
[4] Department of Physics, University of California, Davis, CA95616, USA

Received 13 November 2004, in final form 21 January 2005
Published 4 February 2005
Online at stacks.iop.org/JPhysCM/17/L77

Abstract

The γ–α transition in $Ce_{0.8}La_{0.1}Th_{0.1}$ is measured as a function of applied magnetic field using both resistivity and magnetization. The γ–α transition temperature decreases with increasing magnetic field, reaching zero temperature at around 56 T. The magnetic-field dependence of the transition temperature is quantitatively reproduced by a model that invokes the field and temperature dependence of the entropy of the 4f-electron moments of the γ phase.

(Some figures in this article are in colour only in the electronic version)

The element Ce has attracted considerable theoretical and experimental interest over the past fifty years (see e.g. [1–6] and references therein). One of the most fascinating aspects of its behaviour is the 14.8% collapse in volume that occurs when the face-centred-cubic (fcc) γ phase transforms into the fcc α phase on cooling through $T_{\gamma\alpha} \approx 100$ K at ambient pressure [2, 5, 6]. Although it is generally accepted that the volume collapse is caused by the Ce 4f electrons, a variety of models invoking different physical mechanisms have been put forward. For example, the Mott transition model proposes that the 4f electrons behave as simple band electrons in the α phase but are localized on the Ce ions in the γ phase [6–9]. This approach [7] accounts qualitatively for the reduction in magnetic susceptibility χ that accompanies the volume collapse [2, 10]. However, such a picture is certainly an over-simplification. Neutron scattering [11] and other experiments (see [12–14] and citations therein) suggest a large 4f-electron spectral weight on the Ce site in the α phase. This has been interpreted as evidence for 'localized' f electrons [5, 11]; however, a Ce occupancy of 0.8 ± 0.1 could also be consistent with itinerant f electrons within a narrow-band, tight-binding picture.

The alternative *Kondo volume collapse model* proposes that both the α and γ phases possess highly-correlated 4f electrons, but with very different effective Kondo temperatures [5, 11–13]. In this scheme, the effective Kondo temperature of the γ phase is small, (i.e. less than $T_{\gamma\alpha}$); in the γ phase the properties of the 4f electrons will therefore be almost indistinguishable from those of localized ionic moments. It is thought that the α phase has a relatively large effective Kondo temperature by comparison [11, 14], causing the 4f electrons to be in the mixed-valence regime with significant spd and f hybridization at low temperatures. Consequently one might expect the charge degrees of freedom of α Ce to be describable in terms of itinerant quasiparticles with a large effective mass, a view that is supported by recent optical data [15]. Itinerant quasiparticles are preferable from an energetic standpoint at low temperatures, but the quasi-localized 4f electrons of the γ phase will be favoured on entropic grounds at elevated temperatures [5, 14].

A magnetic field forms a useful probe of the phenomena discussed above. Based on the absolute size of χ in γ Ce and the large fall in χ at the volume collapse [10, 11], an applied field will chiefly affect the energy and entropy of the quasi-localized 4f electrons present in γ Ce; it will have a much smaller effect on the spd conduction electrons in γ Ce and on the itinerant quasiparticles of α Ce [14, 15]. In this study, we have therefore applied steady magnetic fields of up to 27 T and pulsed magnetic fields of up to 57 T to samples of polycrystalline $Ce_{0.8}La_{0.1}Th_{0.1}$. We find that the field B suppresses the γ–α transition temperature, $T_{\gamma\alpha}$, so that it extrapolates to zero temperature at a field $B_{\gamma\alpha}(T \rightarrow 0) \approx 56$ T. This result, and the variation of $T_{\gamma\alpha}$ with B, are in agreement with a simple model of the volume collapse based on entropy arguments [14], originally derived to describe the valence transition in $YbInCu_4$ [16].

There are two reasons to choose $Ce_{0.8}La_{0.1}Th_{0.1}$, rather than pure Ce, for such a study. First, the Th content of the alloy completely suppresses the dhcp β phase [17–19]. By contrast, in pure Ce at ambient pressure the metastable β phase (lifetime $\sim 10^4$ years) is a considerable complication [2]. Successive thermal cyclings of pure Ce lead to 'contamination' of the α phase with varying amounts of β Ce [2, 11]. Moreover, β Ce has a large susceptibility, and the presence of even tiny amounts in the α phase sorely hinders magnetic measurements [2, 11]. Second, the La content of the alloy leads to a $T_{\gamma\alpha}(B = 0)$ that is significantly lower than that in pure Ce [17, 18], enabling the transition to be completely suppressed by available magnetic fields.

Samples are prepared by arc melting the pure metals in an argon atmosphere. The Ce and La used are 99.99% pure and the Th purity is 99.9% (suppliers' figures). The raw materials are arc melted together and then flipped and remelted eight times to ensure sample homogeneity. The uniformity of the composition is further ensured by annealing in vacuum at 676 °C for 11 days. Detailed room-temperature x-ray examinations of several samples showed that only one fcc phase is present (even after thermal cycling through the transition). Both thorium and lanthanum are known to be soluble in Ce at concentrations up to at least 15 at.% [17, 18]; given the extensive annealing times and the reproducibility of the x-ray data, precipitation does not seem to be a problem.

Samples are spark cut from the resulting ingots; electrical contacts are made using 50 μm Pt wires attached using spot welding. Resistance data are recorded in a Quantum Design PPMS (data from 0 to 14 T) or a variable-temperature probe within a 30 T Bitter magnet at NHMFL Tallahassee (data from 0 to 27 T); in both cases, the temperature sensor is a calibrated Cernox resistor in close proximity to the sample. The sample resistance is measured using either a Linear Research LR700 bridge (Bitter magnet experiments) or the resistivity option of the PPMS; the two methods are in good agreement.

Figure 1(a) shows typical resistivity (ρ) versus temperature (T) data with the sample in zero applied magnetic field. The γ–α transition is visible as a reduction in ρ over a range of T that

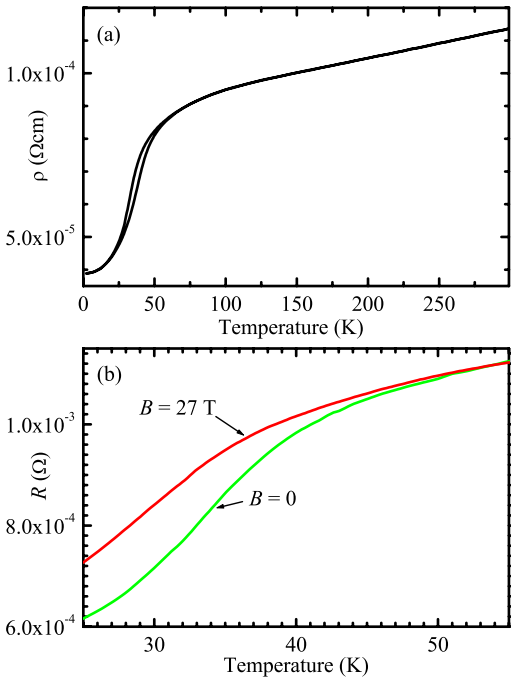

Figure 1. (a) Resistivity ρ of $Ce_{0.8}La_{0.1}Th_{0.1}$ as a function of temperature T with applied magnetic field $B = 0$. The data are recorded by sweeping T at $\sim$1 K min^{-1} from 300 to 2 K and then back to 300 K. Note the hysteresis between down- and up-sweeps of T close to the transition. (b) Resistance R of a $Ce_{0.8}La_{0.1}Th_{0.1}$ sample versus T at $B = 0$ and 27 T. In each case, the sample is warmed above 200 K and then cooled at $\sim$1 K min^{-1} in the stated field.

starts at about 55 K; in agreement with previous measurements of $Ce_{0.8}La_{0.1}Th_{0.1}$ [18], there is hysteresis between data recorded as T falls and those taken as it rises. Although the hysteresis is only clearly visible close to the γ–α transition, there is considerable irreversibility and dissipation involved in the volume collapse; in common with other studies of Ce alloys [17, 18], it is necessary to raise T to above 200 K before each sweep down through the transition to obtain consistent results. In what follows, we concentrate on data acquired as T *falls* from 200 K through $T_{\gamma\alpha}$, so that the transition is always from γ to α.

Zero-field thermodynamic measurements of the $Ce_{0.8}La_{0.1}Th_{0.1}$ samples [20] show that the γ–α transition occurs at $T_{\gamma\alpha}(0) = 47 \pm 1$ K. This corresponds to the centre of the initial downward curve or 'elbow' in $\rho(T)$ as the sample is cooled; this point in the $\rho(T)$ data can be extracted using a variety of methods (e.g. intersection of extrapolations from above and below the transition); in general, such methods give values of $T_{\gamma\alpha}(0)$ within 1 K of each other and within 1 K of the thermodynamic measurements.

Figure 1(b) shows the effect of applied magnetic field B on the γ–α transition; it is clear that the fall in ρ is displaced to lower T. Correspondingly, the fitting and extrapolation procedures give a transition temperature of $T_{\gamma\alpha}(27\,\mathrm{T}) = 40.9 \pm 0.7$ K. Data acquired at several other fields illustrate a similar trend; i.e. $T_{\gamma\alpha}(B)$ is suppressed by increasing B.

Magnetization (M) measurements provide a complementary thermodynamic method for examining the field dependence of the γ–α transition. Figure 2 shows examples of such data recorded at fixed T using an extraction magnetometer inside a 57 T pulsed magnet at NHMFL Los Alamos [21]; before each measurement, the sample is heated to 200 K and then cooled

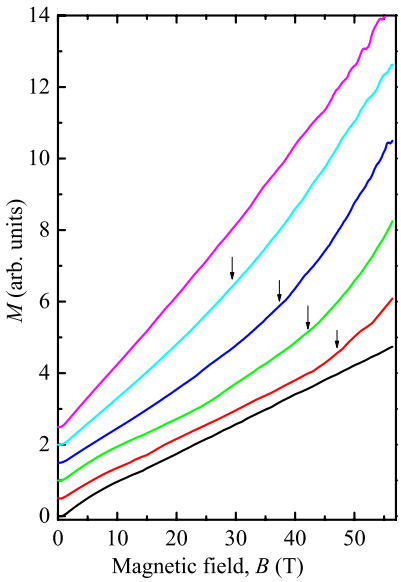

Figure 2. Examples of pulsed-field magnetization (M) data for a $Ce_{0.8}La_{0.1}Th_{0.1}$ sample at fixed temperatures T. Data are shown for $T = 1.6$ K (lowest curve), 25, 30, 35, 40 and 50 K (highest curve); for clarity, the data sets are offset from one another by 0.5 units. The arrows indicate the approximate centre of the transition from lower to higher susceptibility. Before each shot of the pulsed magnet the sample is warmed to above 200 K and then cooled at $\sim$1 K min^{-1} to the required temperature.

slowly ($\sim$1 K min^{-1}) to the required temperature. Data for $T > T_{\gamma\alpha}$ (e.g. the $T = 50$ K data in figure 2) show a relatively large susceptibility $\chi = \mathrm{d}M/\mathrm{d}H$, in agreement with expectations for the γ phase [10, 11, 17]. For $T \ll T_{\gamma\alpha}$, unambiguously in the α phase (e.g. the $T = 1.6$ K data in figure 2), M increases more slowly, consistent with the small χ observed by others [10, 17]. However, at intermediate T, there is a distinct 'elbow' or change in slope, consistent with a transition from a large χ (at high B) to a smaller χ (at low B). We associate this change in χ with a field-induced phase change from γ (high B) to α (low B).

Although the γ–α transition in $Ce_{0.8}La_{0.1}Th_{0.1}$ is first order [18, 20], the 'elbow' in the $M(B)$ data (e.g. figure 2, $T = 35$ K) is rather broad compared to the 'step' in M or resistance observed at the valence transition in $YbInCu_4$ [16]. There are two reasons for this difference. First, Ce and its alloys are known to exhibit 'sluggish kinetics' [22], in which dissipative processes with long time constants act to broaden the transition when a thermodynamic variable (such as B) is changed rapidly. Second, in contrast to the pure single-crystal $YbCuIn_4$ samples of [16], our $Ce_{0.8}La_{0.1}Th_{0.1}$ samples are polycrystalline. Consequently, not all Ce lattice sites are equivalent, and there will exist a non-uniform distribution of stress, forcing different Ce sites to respond with different time constants, or at a range of fields.

The field position of the transition is taken to be the intersection of linear extrapolations of the low- and high-B gradients (arrows indicating these positions are shown for the data sets in figure 2); in this way, transition fields $B_{\gamma\alpha}(T)$ can be extracted from $M(B)$ data at a number of fixed T.

The transition temperatures $T_{\gamma\alpha}(B)$ from the fixed-B $\rho(T)$ measurements and the transition fields $B_{\gamma\alpha}(T)$ obtained from the fixed-T $M(B)$ experiments are summarized in figures 3(a) and (b). Data from the two techniques may be distinguished as follows. Owing to the width of the transition, the $B_{\gamma\alpha}(T)$ points from the $M(B)$ experiments have quite a large

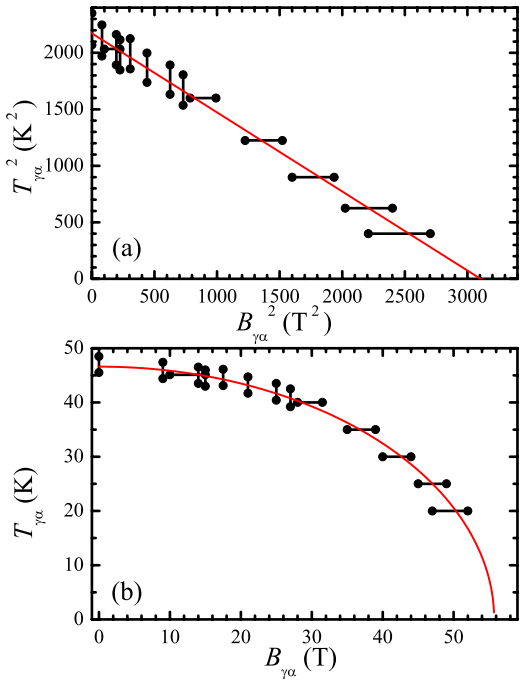

Figure 3. Values of $B_{\gamma\alpha}(T)$ from the $M(B)$ experiments at fixed T (horizontal error bars) and values of $T_{\gamma\alpha}(B)$ from $\rho(T)$ experiments at fixed B (vertical error bars) plotted as T^2 versus B^2 (a) and in linear units (b). The line in (a) and the curve in (b) represent equation (2) with $B_{\gamma\alpha}(T \to 0) = 56$ T and $T_{\gamma\alpha}(B = 0) = 46.6$ K.

field uncertainty[5]. These data are therefore plotted as horizontal error bars. On the other hand, the $T_{\gamma\alpha}(B)$ values from the $\rho(T)$ data possess a relatively large temperature uncertainty, so that they are represented by vertical error bars. In spite of the differences between the measurement techniques, there is reasonable agreement between the two sets of data shown in figure 3. Note also that the data lie on a straight line when plotted in the form $B_{\gamma\alpha}^2$ versus $T_{\gamma\alpha}^2$ (figure 3(a)).

To understand the variation of the γ to α transition with B and T, we turn to the magnetic entropy model of Dzero *et al* [14]. This is based on the premise that the low-T phase possesses an energy scale characterized by an effective Kondo temperature $T_{\mathrm{K}\alpha}$ that is much larger than the corresponding energy scale for the high-T phase, $T_{\mathrm{K}\gamma}$, i.e. $T_{\mathrm{K}\alpha} \gg T_{\mathrm{K}\gamma}$. This view is supported by variety of experiments that suggest $k_{\mathrm{B}}T_{\mathrm{K}\alpha} \sim 80$–$170$ meV and $k_{\mathrm{B}}T_{\mathrm{K}\gamma} \sim 5$–$8$ meV (see [5, 11–14] and references therein). The large value of $T_{\mathrm{K}\alpha}$ means that the free energy $F_\alpha(B, T)$ of the α phase will vary only slowly with B. By contrast the quasi-localized 4f electrons of the γ phase will couple strongly to B, producing a large negative contribution to the γ phase's free energy, $F_\gamma(B, T)$. This distinction is emphasized [14] by writing $F_\gamma = E_0 - TS(B, T)$, where E_0 indicates the contribution of the spd electrons and $S(B, T)$ is the entropy associated with the 4f multiplet of angular momentum J, Landé g-factor g_J. Hence, the contribution of the 4f moments to $F_\gamma(B, T)$ can be written

$$TS(B, T) = -T \log_{\mathrm{e}} \left(\sum_{m_{\mathrm{J}}=-J}^{\mathrm{J}} \exp\left[-\frac{g_J \mu_{\mathrm{B}} B m_{\mathrm{J}}}{T} \right] \right). \tag{1}$$

[5] For $\lesssim$15 K, $B_{\gamma\alpha}$ rapidly approaches the upper limit of the magnet used. Thus, the broadness of the γ–α transition prevents us from assigning $B_{\gamma\alpha}$ values with any confidence for $T \leqslant 15$ K.

The phase boundary is defined by $F_\gamma(B, T) = F_\alpha(B, T)$. Owing to the fact that both $F_\alpha(B, T)$ and E_0 will vary relatively slowly with B and T compared to $TS(B, T)$, the approximate condition for the boundary becomes $TS(B, T) \approx$ constant. With this constraint, manipulation of equation (1) [14] yields

$$\left(\frac{B_{\gamma\alpha}}{B_{\gamma\alpha}(T \to 0)}\right)^2 + \left(\frac{T_{\gamma\alpha}}{T_{\gamma\alpha}(B = 0)}\right)^2 \approx 1, \tag{2}$$

for the γ–α phase boundary; i.e. a plot of $B^2_{\gamma\alpha}$ versus $T^2_{\gamma\alpha}$ should yield a straight line.

The line in figure 3(a) is a fit of the data to equation (2) with $B_{\gamma\alpha}(T \to 0)$ and $T_{\gamma\alpha}(B = 0)$ as adjustable parameters. The values obtained were $B_{\gamma\alpha}(T \to 0) = 56 \pm 1$ T (see footnote 5) and $T_{\gamma\alpha}(B = 0) = 46.6 \pm 1$ K. A consistency check of these values can be obtained by again setting $TS(B, T)$ equal to a constant and examining equation (1) in the limits $B = 0$ and $T \to 0$; this produces

$$\frac{k_B T_{\gamma\alpha}(B = 0)}{\mu_B B_{\gamma\alpha}(T \to 0)} = \frac{g_J J}{\log_e(2J + 1)} \approx 1.20, \tag{3}$$

where we have inserted the known values [10, 11] $J = \frac{5}{2}$ and $g_J = \frac{6}{7}$ for the quasi-localized f electrons of γ Ce. Using the fit parameters derived from figure 3, the experimental ratio $k_B T_{\gamma\alpha}(B = 0)/\mu_B B_{\gamma\alpha}(T \to 0)$ is 1.24, within a few per cent of the prediction of equation (3).

The success of the model of [14] in describing the $Ce_{0.8}La_{0.1}Th_{0.1}$ data demonstrates that the free-energy contribution of the 4f moments is the dominant cause of the γ–α transition; other contributions (such as phonon entropy) appear to be of minor importance. This is in agreement with the proposal, based on a qualitative assessment of phonon spectra, that the entropy of the 4f moments determines the structural phase of the related alloy $Ce_{0.9}Th_{0.1}$ [19]. The good fits to the data of figure 3 provided by equations (2) and (3) add a *quantitative* justification to this argument. By contrast, a greater role phonon entropy in the γ–α transition was inferred from recent high-pressure neutron scattering experiments on pure Ce [23]. However, the latter data were recorded at much higher temperatures (260–300 K) than those used here; at $T \sim 300$ K, the entropy of the phonon system will be rather larger [24]. A further difference could be due to the fact that alloying alters the phonon spectrum of Ce [20, 25]. Nevertheless, in the current case of $Ce_{0.8}La_{0.1}Th_{0.1}$, it is clear that the phonon system is largely irrelevant; the data show unambiguously that the γ–α transition couples to the magnetic field and that it can be suppressed by very high fields.

Finally, we remark that in contrast to $YbCuIn_4$ [14, 16], there is an f moment at almost every lattice site in $Ce_{0.8}La_{0.1}Th_{0.1}$. In such a system, which shows many of the traits of correlation, it is very interesting that the moments of the γ phase behave almost identically to isolated Ce ions, enabling equations (1)–(3) to describe the data. Consequently, the γ–α transition is driven mainly by the fact that entropy considerations favour 4f electrons that are effectively localized at high T and B (and at low pressures [5]). The delocalization of the f electrons manifested as itinerant quasiparticle behaviour [15] of the α phase is energetically favourable from zero-point-energy considerations, but it is costly on entropic grounds. Thus, the α phase is stable at low T and B (and at high pressures).

In summary, we have measured the γ–α transition in $Ce_{0.8}La_{0.1}Th_{0.1}$ as a function of applied magnetic field using resistivity and magnetization. The transition temperature is suppressed by increasing magnetic field, extrapolating to absolute zero at around 56 T. The magnetic field-temperature phase boundary is adequately fitted by a simple model [14] of the field and temperature dependence of the entropy of the localized f-electron moments in the γ phase. Many substances undergo structural phase transitions which are thought to involve f electrons changing from 'localized' to itinerant behaviour (e.g. Plutonium [26]). On the basis

of the work reported here, it seems likely that the application of high magnetic fields to such substances will yield valuable information about the role of the f electron system in stabilizing the various structural phases.

This work is supported by the US Department of Energy (DOE) under Grant No. LDRD-DR 20030084 'Quasiparticles and Phase Transitions in High Magnetic Fields: Critical Tests of Our Understanding of Plutonium', the National Science Foundation (NSF) (grant DMR-0433560) and the National Nuclear Security Administration under the Stewardship Science Academic Alliances program through DOE grant DE-FG03-03NA00066. It was carried out at the National High Magnetic Field Laboratory, which is supported by the NSF, the State of Florida and DOE. We thank Stan Tozer for enthusiastic experimental assistance.

References

[1] Lawson A W and Tang T-Y 1949 *Phys. Rev.* **76** 301
[2] Koskenmaki D C and Gschneider K A 1978 *Handbook on the Physics and Chemistry of Rare Earths* ed K A Gschneider and L Eyring (Amsterdam: North-Holland) p 337
[3] Malterre D, Grioni M and Baer Y 1996 *Adv. Phys.* **45** 299
[4] Nikolaev A V and Michel K H 2002 *Phys. Rev.* B **66** 054103
[5] Laegsgaard J and Svane A 1999 *Phys. Rev.* B **59** 3450
[6] Held K, McMahan A K and Scalettar R T 2001 *Phys. Rev. Lett.* **87** 276404
[7] Johansson B 1974 *Phil. Mag.* **30** 469
[8] Svane A 1996 *Phys. Rev.* B **53** 4275
[9] Johansson B, Abrikosov I A, Aldén M, Ruban A V and Skriver H L 1995 *Phys. Rev. Lett.* **74** 2335
[10] Koskimaki D C and Gschneider K A 1975 *Phys. Rev.* B **11** 4463
[11] Murani A P, Bowden Z A, Taylor A D, Osborn R and Marshall W G 1993 *Phys. Rev.* B **48** 13981
[12] Liu L Z, Allen J W, Gunnarsson O, Christensen N E and Andersen O K 1992 *Phys. Rev.* B **45** 8934
[13] Allen J W and Liu L Z 1992 *Phys. Rev.* B **46** 5047
[14] Dzero M O, Gor'kov L P and Zvezdin A K 2000 *J. Phys.: Condens. Matter* **12** L711
[15] van der Eb J W, Kuz'menko A B and van der Marel D 2001 *Phys. Rev. Lett.* **86** 3407
[16] Immer C D *et al* 1997 *Phys. Rev.* B **56** 71
[17] Grier B H, Parks R D, Shapiro S M and Majkrzak C F 1981 *Phys. Rev.* B **24** 6242
[18] Thompson J D, Fisk Z, Lawrence J M, Smith J L and Martin R M 1983 *Phys. Rev. Lett.* **50** 1081
[19] Manley M E *et al* 2003 *Phys. Rev.* B **67** 014103
[20] Lashley J C 2003 unpublished data
[21] Singleton J, Mielke C H, Migliori A, Boebinger G S and Lacerda A H 2004 *Physica* B **346/347** 614
[22] Gschneidner K A *et al* 1999 *J. Phase Equilib.* **20** 612
[23] Jeong I-K *et al* 2004 *Phys. Rev. Lett.* **92** 105702
[24] Dove M T 2003 *Structure and Dynamics* (Oxford: Oxford University Press) chapter 9
[25] Clinard F W 1969 *J. Appl. Phys.* **40** 3067
[26] Lashley J C *et al* 2003 *Phys. Rev. Lett.* **91** 205901